Exploring force allocation control of over actuated vehicles

Johannes Edrén

Licentiate Thesis

TRITA AVE 2011:80
ISSN 1651-7660

Postal address	Visiting Address	Telephone	Telefax	Internet
KTH Vehicle Dynamics SE-100 44 Stockholm, Sweden	Teknikringen 8 Stockholm	+46 8 790 6000	+46 8 790 9290	www.kth.se

Abstract

As the concern for environmental changes and diminishing oil resources grows more and more, the trend of new vehicle concepts now includes full electric or partly electric propulsion systems. The introduction of electric power sources enables more advanced motion control systems due to electrification of the vehicle's actuators, such as individual wheel steering and in wheel hub motors. This can enable a control methodology that uses different chassis control strategies into a system that will be able to fully utilise the vehicle. Due to this, future vehicles can be more optimised with respect to energy consumption, performance and active safety.

Force allocation control is a method that distributes the wheel forces to produce the desired response of the vehicle. In order to evaluate if this methodology can be implemented in future series production vehicles, the aim of this work is to explore how force allocation control can be utilised in a real vehicle to improve vehicle dynamics and safety.

In order to evaluate different approaches for generic vehicle motion control by optimization, modelling and simulation in combination with real vehicle experiments will be needed to fully understand the more complex system, especially when actuator dynamics and limitations are considered. The use of a scale prototype vehicle represents a compromise between development cost, efficiency and accuracy, as it allows realistic experiments without the cost and complexity of full vehicle test. Moreover since the vehicle is unmanned it allows studies of at-the-limit situations, without the safety risks in full vehicle experiments.

A small scale prototype vehicle (Hjulia) has been built and equipped with *autonomous corner module* functionality that enables individual control of all wheels. A cost effective force allocation control approach has been implemented and evaluated on the prototype vehicle, as well as in vehicle simulation. Results show improvement of stopping distance and vehicle stability of a vehicle during split-μ braking. The aspects of vehicle dynamic scaling are also discussed and evaluated, as it is important to know how the control implementation of small scale prototype vehicles compares with full size vehicles. It is shown that there is good comparison between vehicles of different scales, if the vertical gravitational acceleration is adjusted for. In Hjulia, gravity compensation is solved by adding a specific lifting rig.

Studies of vehicles considering optimal path tracking and available actuators are also made to evaluate control solutions of evasive manoeuvres at low and high friction surfaces. Results show differences in how the forces are distributed among the wheels, even though the resulting global forces on the vehicle are approximated to be scaled by friction. Also it is shown that actuator limitations are critical in at-the-limit situations, such as an obstacle avoidance manoeuvre. As a consequence these results will provide good insights to what type of control approach to choose to handle a safety critical situation, depending on available actuators.

The built prototype vehicle with implemented force allocation control has shown to be a useful tool to investigate the potential of control approaches, and it will be used for future research in exploring the benefits of force allocation control.

Acknowledgements

This research has been carried out at the division of Vehicle Dynamics at KTH, the Royal Institute of Technology, in Stockholm, Sweden. The work is financed by SHC, the Swedish Hybrid Vehicle Centre and the Swedish Energy Agency, which is greatly acknowledged.

I would like to express gratitude to all people involved in this project. My supervisors, Professor Annika Stensson Trigell, Assistant Professor Jenny Jerrelind and Associate Professor Lars Drugge at KTH. Fellow co-author Mats Jonasson at Volvo Car Corporation (VCC) for very exciting joint work. Johan Andreasson and Peter Sundström at Modelon, Professor Bengt Jacobson at Chalmers. People in the steering group: Oskar Wallmark, Leo Laine, Mats Leksell, Olof Noréus, Gunnar Olsson and Matthjis Klomp. Fellow colleagues at KTH: Daniel Wanner, Mikael Nybacka, Sigvard Zetterström, Malte Rothhämel and Jonas Jarlmark Näfver. Also former fellow colleagues: Adam Rehnberg, Andreas Erséus, Fredrik Svahn, Markus Agebro and Sanna Edberg. Kent Lindgren and Danilo Prelevic at the MWL laboratory have been extremely helpful during the construction of the vehicle and measuring equipment.

Last but no least, thanks to all of my friends and family for support and motivation.

Stockholm 2011

Johannes Edrén

Dissertation

A Licentiate of Technology is an intermediate Swedish academic degree that can be obtained half-way between the MSc and PhD. While less formal than a Doctoral Dissertation, examination for the degree includes writing a thesis and a public presentation with an invited discussion leader.

This licentiate thesis consists of two parts. The first part gives an overview of the research with a summary of the performed work. The second part collects the following scientific papers, which are referred to in the text by their short version, **Paper A**. etc:

The following publications are included in this thesis:

A J. Edrén, M. Jonasson, A. Stensson Trigell, L. Drugge and J. Jerrelind, "The development of a down-scaled over-actuated vehicle equipped with autonomous corner module functionality", FISITA Proceedings 2010, paper F2010B056, 2010.

Edrén designed and built the vehicle and wrote the paper. Stensson Trigell and Jonasson specified the problem. Jonasson, Jerrelind, Stensson Trigell and Drugge supervised the work and assisted with writing the paper. Edrén presented the paper as a poster at FISITA 2010 World Automotive Congress, May 30-June 4, Budapest, Hungary, 2010.

B J. Edrén, J. Jerrelind, A. Stensson Trigell and L. Drugge, "Implementation and evaluation of force allocation control of a down-scaled prototype vehicle with wheel corner modules", submitted for publication, 2011.

Edrén developed and implemented the prototype vehicle controller and simulation model, performed the experiments and wrote the paper. Jerrelind, Stensson Trigell and Drugge supervised the work and assisted with result evaluation and with writing the paper.

C J. Edrén, P. Sundström, M. Jonasson, B. Jacobson, J. Andreasson and A. Stensson Trigell, "Road friction effect on the optimal vehicle control strategy in two critical manoeuvres", submitted for publication, 2011.

Edrén performed simulations and wrote the paper. Sundström assisted with model programming. Jonasson, Jacobson and Andreasson assisted with result evaluation criteria and model specification. Stensson Trigell supervised the work and assisted with proofreading the paper.

The author has contributed to other publications which are not incorporated in this thesis, these are as follows:

D A. Rehnberg, J. Edrén, M. Eriksson, L. Drugge, A. Stensson Trigell, "Scale model investigation of articulated frame steer vehicle snaking stability", International Journal of Vehicle System Modelling and Testing, Vol. 6, No. 2, pp. 126-144, 2011.

Rehnberg conceived the idea, specified the requirements for the test vehicle, performed the theoretical analysis and wrote the paper, Edrén and Eriksson designed and built the test vehicle and performed all measurements. Drugge assisted with the vehicle design specification, the result analysis and writing of the paper. Stensson Trigell supervised the work and assisted by proofreading the paper.

E J. Edrén, M. Jonasson, A. Nilsson, A. Rehnberg, F. Svahn, A. Stensson Trigell, ”Modelica and Dymola for education in vehicle dynamics at KTH”, Paper MODEL09_0112_F1, In Proceedings from 7th Modelica Conference 2009, Como, Italy, 2009.

The paper was written jointly, Edrén put the material together.

Contents

1. Introduction

1.1 Background

In the beginning of the automotive history, before the internal combustion engine became the dominant mode of propulsion, cars were fitted with many different kinds of propulsion systems, such as steam, electric and gasoline. Electric cars were common and car manufacturers experimented a lot with drive systems and configurations. For example Ferdinand Porsche pioneered with electric in wheel hub motors in a car as early as 1901, that can be categorized as a hybrid electric vehicle (HEV) [1]. Even the first car driven on all four wheels was a HEV, with in wheel hub motors.

As the concern for environmental changes and diminishing oil resources grows more and more, the trend of new vehicle concepts now goes back to the early days with full electric or partly electric propulsion. But in comparison the ability to control these systems are now much more promising thanks to the computer revolution. Seemingly endless configuration possibilities come with an increased set of available actuators, such as individual steering actuators and in wheel hub motors.

The majority of road vehicles today are steered directly by a mechanical linkage from the steering wheel to the steered axle. On a vehicle with four wheels, such as a passenger car, the front axle is often the preferred axle to be steered. When studying vehicle behaviour the resulting forces from the wheels can be added together to the three global inputs to the vehicle; longitudinal force, lateral force and yaw torque, in order to get a system that is easier to understand. These three inputs are mainly a function of the driver input. For longitudinal force the accelerator and braking pedal has been the control input. For lateral force and yaw torque, the steering wheel. The system is however not fully determined as two input controls three degrees of freedom.

The response in yaw and lateral velocity from steering wheel input is determined by the physical dimensions and properties of the vehicle such as wheel base, vehicle mass, tyre characteristics etc. These parameters are governing the vehicle behaviour and are hard to alter without physically changing the vehicle considerably. However with an over actuated vehicle the possibility to influence the response will increase. A system is considered to be over actuated if there are more actuators than degrees of freedom (DOF) that is to be controlled.

Considerable amount of work has been presented in the field of control and safety of over actuated vehicles, see for example Andreasson et al [2]. The domain of over actuated control also goes beyond the automotive world, such as the aerospace and robotics. The trend is to increase the number of control functions. Each function is typically developed to tackle a particular control problem isolated from other control problems. Since the control functions do not collaborate much, the need of a supervisory control has gained a lot of interest. Active research on this topic among many others is presented in [3-5] where electromechanical actuation is considered.

In the late 1970s, anti-lock brake systems (ABS) [6] were introduced which resulted in that the car became an over actuated system. Instead of applying a predefined brake force distribution to all wheels, the wheels are prevented to be locked, by controlling wheel brake forces individually, thus affecting vehicle stability and steer ability. This also gives the possibility to use the brake actuation to add or subtract yaw torque which pawed the way for more advanced chassis controller systems such as the Electronic stability program (ESP) [7]. Many of these systems have for a long time only utilised engine torque and friction brake actuators as the main control output. However there are now systems which starts to incorporate electric power assisted steering (EPAS) and rear axle steering (RAS) to the ESP system.

With individual wheel control, the ability of applying requested forces such as for example lateral tyre forces, is extended. Load distribution enabling for better utilisation of the tyres is made possible. However with more actuators there exists a higher risk of faults, but at the same time the ability to remedy these faults is higher due to the multiple outputs [8-9].

One example of an over actuated vehicle suitable for individually wheel control is the autonomous corner module (ACM). This is a concept invented by S. Zetterström in 1998 [10]. The name autonomous indicates that the wheel forces and kinematics are individually controlled, supporting a common task [10-12]. More in detail the ACM concept is a modular based suspension system that includes all features of wheel control, such as control of steering, wheel torques, wheel loads and camber individually. Multiple outputs to control the wheel and its functions enabling, what is called over actuation.

For any system with over actuation, there exists a task of calculating the appropriate control outputs to all the actuators. It can be done, for example for a car with all wheel steering, by simply fixing the rear wheel steering angles like a normal car, not fully utilise the rear steering actuators. But this approach does not really take full advantage of the vehicle, meaning there is a more optimal way of controlling the actuators, maximising vehicle performance.

Looking at the vehicle as a simple box, where each corner is considered a point to apply force to, the forces of the vehicle can be seen in different "levels". At a global level only the total resulting forces acting upon the chassis are considered. For example the global longitudinal force F_x is the sum of all the longitudinal corner forces f_{xc}. Figure 1.3 shows how global forces relate to tyre and actuator forces. Having this mindset, vehicle control is performed on the global level, and force allocation is required to calculate the appropriate actuator outputs fulfilling the result at the global level. The number of actuator solutions giving the same global results is however infinite. To solve which solution that is most appropriate in each situation cost functions and constraints has to be added. Energy consumption cost for example will enable the algorithm to find the most energy efficient solution.

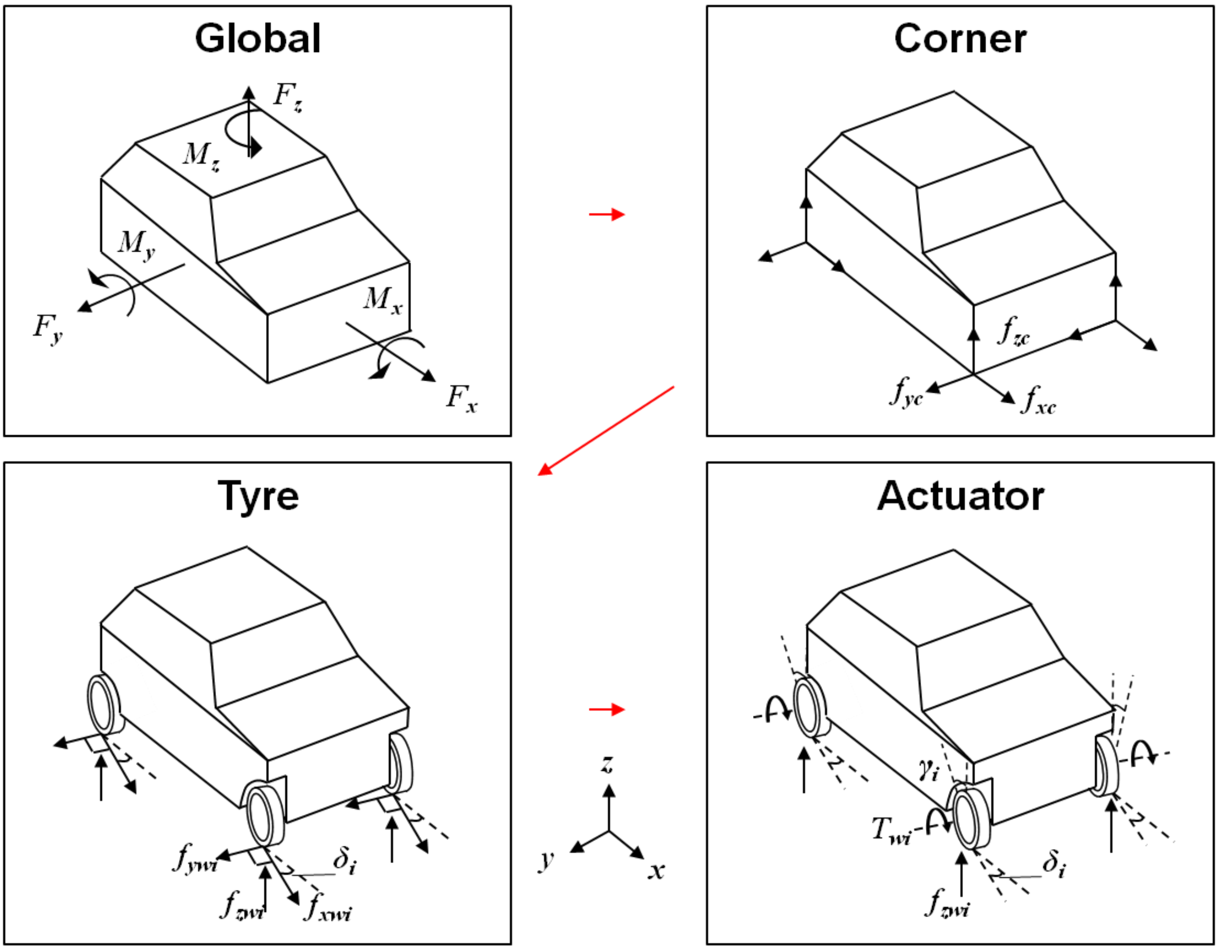

Figure 1.3. Forces on a vehicle presented at global, corner, tyre and actuator level.

Furthermore, as the amount of available actuators increases, the allocator cost function specification is important, since it strongly determines the vehicle behaviour. It is shown that performance can be considerably enhanced by shifting the weights [13-14]. Therefore, rather than eliminating situation recognition as a problem, it has to be redefined as a shift of priorities. For example, the priorities during limit conditions are needed to be studied in more detail, such as shifting the balancing between the different sub costs.

In order to evaluate different approaches for generic vehicle motion control by optimization, modelling and simulation in combination with real vehicle experiments will be needed to fully understand the more complex system, especially when actuator dynamics and limitations are considered. However full scale vehicles implemented with force allocation possibilities would be expensive. The use of a scale prototype vehicle represents a compromise between development cost, efficiency and accuracy, as it allows realistic experiments without the cost and complexity of full vehicle test. Moreover since the vehicle is unmanned it allows studies of at-the-limit situations, without the safety risks in full vehicle experiments.

In order to be able to evaluate the most promising solutions for industrial applications, the methodology suggested here is to *combine theory, modelling and simulation with experiments using a purposely developed scaled prototype vehicle*.

1.2 Research question

The scope of this research is to further utilise the force allocation approach, where sensor uncertainties, time delays and actuator limitations etc. are considered. The long term aim is to identify what aspects that are crucial to make optimal generic motion control techniques more suitable for industrial applications. More specifically, the research question for this thesis work is:
"How can force allocation be utilised in a real vehicle to improve vehicle dynamics and safety?"

Investigated areas are optimal use of actuators in limit handling situations when using non ideal sensors, estimated vehicle parameters and distribution of computing resources. The methodology is to combine theory, modelling and simulation with experiments using a purposely developed scaled prototype vehicle.

1.3 Outline of thesis

This thesis is divided into four main parts. The first part (Chapter 2) is describing the approach of using scaling to understand how control of a small scale vehicle can be compared to a full-size vehicle, using a vehicle dynamic simulation study. Second part (Chapters 3 and 4) describes the scaled prototype vehicle that has been developed in this work, and the implemented control approach. The third part (Chapter 5) is about optimisation in an at-the-limit situation performed on a vehicle simulation model that includes actuator constraints, to study the behaviour of the solution of an optimisation algorithm controlling a vehicle in a standardised manoeuvre. Finally, the work is summarised and discussed (Chapters 6 to 9).

2. Scaling of vehicle dynamics

2.1 Introduction

As mentioned earlier small scale testing is a very useful tool when studying vehicle behaviour. One example of work with a down-scaled vehicle for studying the dynamic behaviour of articulated vehicles is made in **Paper D** where a wheel loader was built and tested for so called “snaking” stability.

Of course there are limitations of what can be studied with small scale vehicles, especially if dimension scaling is considered. One example is high frequency dynamics, such as noise and comfort, which is difficult to reproduce. To study the vehicle chassis controller however, it is mainly in-plane rigid body dynamics that is of importance.

If a scale model is meant to replicate a car driving in steady state cornering, (constant speed, constant turning radius), with the vehicle speed according to length scale, the centripetal acceleration will have to be scaled by the same amount, according to dimensional analysis similar to [15]. Studying the cornering forces generated by the wheels of the vehicle, the resulting maximum friction forces, due to the scaled normal loads, also have to be scaled. The friction force is depending on wheel load and friction coefficient. To limit this force the choice is to either scale the friction coefficient or the vertical load.

The easiest way is to alter the road/tyre friction coefficient μ, and that will give reasonable dynamics of the planar motion. But the distribution of vertical wheel loads will still be unrealistic. The vehicle will never be able to be driven close to the limit of roll over or wheel lift. Altering the vertical forces is of course complicated since this force is given by vehicle mass and the earth’s gravity. As the vehicle mass is critical to the planar motion of the vehicle and the gravity is very difficult to alter, the choice is to cancel out an amount of the gravitational pull by lifting the vehicle in its centre of gravity. This lifting can for example be achieved by a very long bungee-cord, or by a lifting rig with wheels that only take up some of the vertical load, see **Papers A** and **B**.

Another method is to combine lower friction coefficient with the centre of gravity placed higher in the vehicle. This will allow more weight transfer but with the drawback of influencing the inertia of the roll and pitch motion.

The scaling strategy chosen is based on [15]. In this example the chosen scale is 1/10 for simplicity and all parameters are defined in Nomenclature.

Starting with the length scaling factor φ_l:

$$\varphi_l = \frac{l_1}{l_0} = 10 \tag{1}$$

l_1 is is a characteristic length of the full scale and l_0 a characteristic length of the scale model. In the same way a time scaling factor is introduced:

$$\varphi_t = \frac{t_1}{t_0} = 1 \tag{2}$$

Choosing the values of these scaling factors together with the density scaling factor:

$$\varphi_\rho = \frac{\rho_1}{\rho_0} = 1 \tag{3}$$

The resulting scaling factors for the rest of the parameters for speed, acceleration, mass, inertia, force, torque, suspension stiffness, and suspension damping, follows:

$$\varphi_v = \frac{\varphi_l}{\varphi_t} = 10 \tag{4}$$

$$\varphi_a = \frac{\varphi_l}{\varphi_t^2} = 10 \tag{5}$$

$$\varphi_m = \varphi_\rho \cdot \varphi_l^3 = 10^3 \tag{6}$$

$$\varphi_I = \varphi_m \cdot \varphi_l^2 = 10^5 \tag{7}$$

$$\varphi_F = \varphi_m \cdot \varphi_a = 10^4 \tag{8}$$

$$\varphi_T = \varphi_F \cdot \varphi_l = 10^5 \tag{9}$$

$$\varphi_c = \frac{\varphi_F}{\varphi_l} = 10^3 \tag{10}$$

$$\varphi_d = \frac{\varphi_F}{\varphi_v} = 10^3 \tag{11}$$

2.2 Vehicle model study

To be able to understand the scaling effects of vehicle dynamics, for vehicle chassis control evaluation, a vehicle model in MATLAB [16] was developed with the ability to change the scale, changing the vital parameters according to characteristic length.

The vehicle model is a 6 degree of freedom (DOF) model with a basic nonlinear magic formula (MF) tyre model for pure slip conditions [17]. The in-plane motion is described by longitudinal (x), lateral (y) and yaw (ψ) DOFs, and the out-of-plane motion is described by vertical (z), pitch (Θ) and roll (φ) DOFs. The out of plane dynamics is guided by springs, dampers and anti-roll bars. Figure 2.1 show the vehicle model visualised in MATLAB. Parameters for the two vehicles (full-scale vehicle and 1/10-scale vehicle) are presented in Table 2.1. Note that the MF tyre stiffness is not scaled. The resulting forces from the tyre model will however be scaled due to the fact that the vertical forces are scaled.

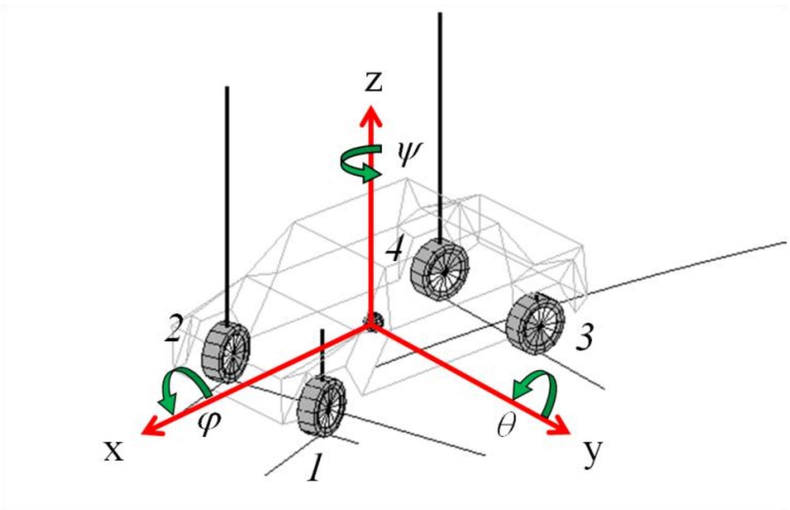

Figure 2.1. Six DOF simulation model illustrated with lateral, longitudinal and vertical tyre force visualisation. Chassis motion ($x,y,z,\psi,\Theta,\varphi$).

Table 2.1. Vehicle parameters for the two models analysed.

Description	Parameter	Full-scale Value	1/10-scale Value	Unit
Vehicle mass	m	2131	2.131	[kg]
Roll inertia	J_{xx}	764	0.00764	[kgm^2]
Pitch inertia	J_{yy}	3477	0.03477	[kgm^2]
Yaw inertia	J_{zz}	3925	0.03925	[kgm^2]
CoG to front axle distance	f	1.3	0.13	[m]
CoG to rear axle distance	b	1.47	0.147	[m]
Wheel track distance	wb	1.5	0.15	[m]
CoG to ground distance	h	0.5	0.05	[m]
Front spring stiffness	c_1, c_2	33000	33	[N/m]
Rear spring stiffness	c_3, c_4	56000	56	[N/m]
Front Stabilizer stiffness	c_{12}	20006	20.006	[N/m]
Rear Stabilizer stiffness	c_{34}	16088	16.088	[N/m]
Front damping coefficient	d_1, d_2	4500	4.5	[Ns/m]
Rear damping coefficient	d_3, d_4	3500	3.5	[Ns/m]
MF Tyre Front stiffness	B_1, B_2	19.2	19.2	[-]
MF Tyre Rear stiffness	B_3, B_4	21.3	21.3	[-]
MF Tyre Shape factor	C_1, C_2, C_3, C_4	1	1	[-]
Relaxation length	L_1, L_2, L_3, L_4	0.15	0.015	[m]

To evaluate the scale vehicle model both vehicles are subjected to a ramp steering event where the vehicle initially travels along a straight line and after 1 s the steering starts the turn. The initial vehicle speed is scaled, as is the constant longitudinal tyre force driving the front wheels. The simulation for both the scaled and the full-scale vehicles stops after 10 s.

Figure 2.2 shows the resulting path of the full-scale vehicle and the 1/10-scaled vehicle. The path results show as expected that the vehicle path is scaled with the resulting path position being exactly 1/10 smaller for the 1/10-scaled vehicle in relation to the full-scale vehicle.

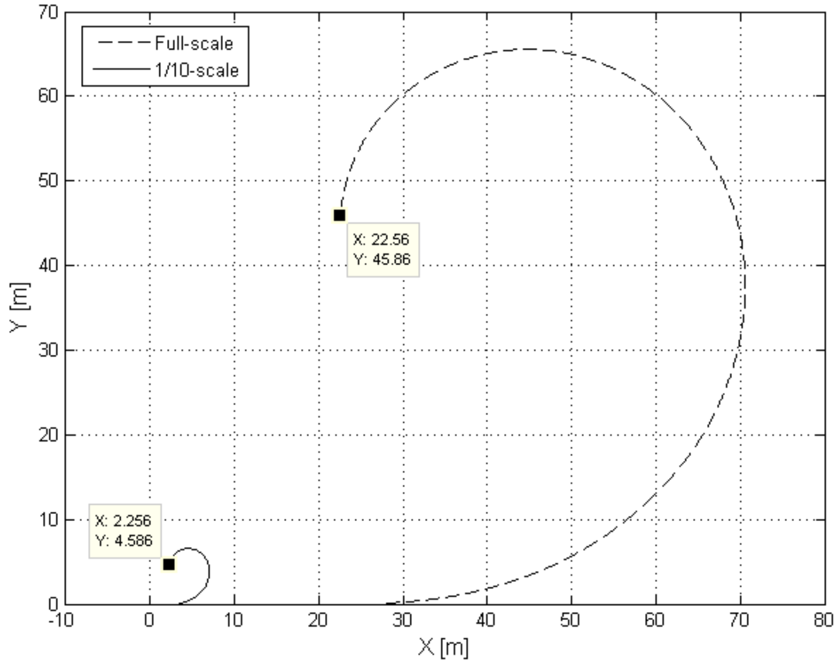

Figure 2.2. Comparison between full-scale and 1/10-scaled simulations.

Studying the tyre forces, see Figure 2.3, it can be seen that the force magnitudes are scaled by the factor $\varphi_F = 10^4$. Roll and pitch angles are also identical throughout the manoeuvre. The numbers 1-4 refers to the respective wheel corners as indicated earlier in Figure 2.1.

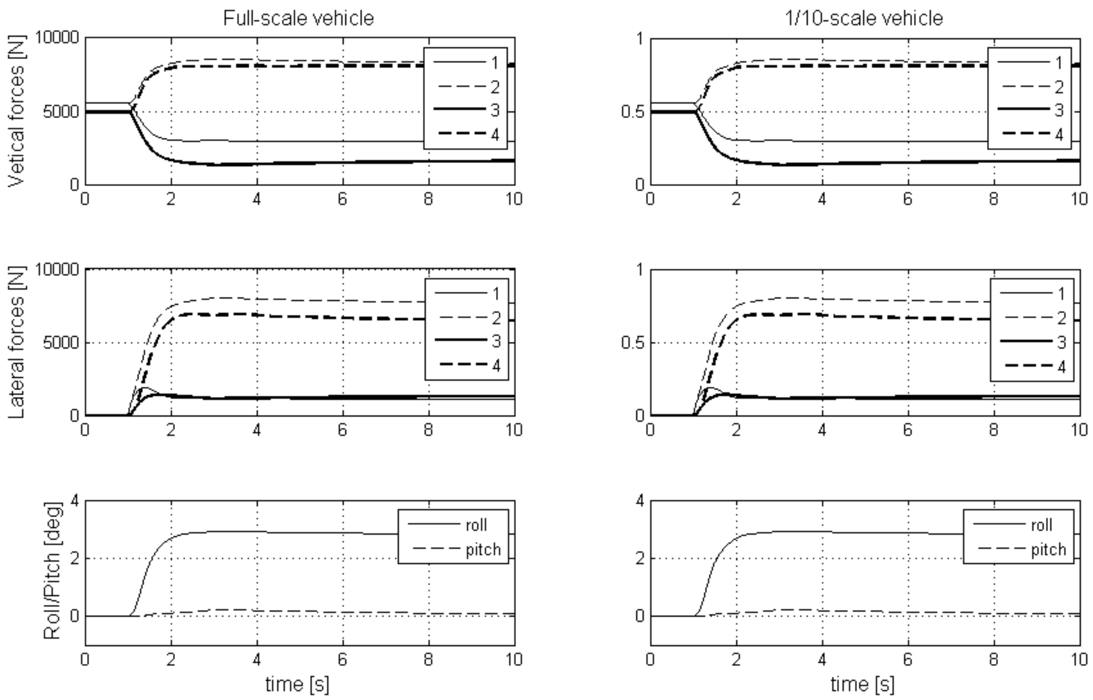

Figure 2.3. Simulation result of vertical and lateral tyre forces, body roll and pitch angles for the full-scale vehicle compared with the 1/10-scale vehicle.

3. The over actuated scaled prototype vehicle

The down-scaled vehicle developed in this work has autonomous corner module functionality and is referred to as “Hjulia”, see Figure 3.1. Hjulia is designed to be a low cost tool to be able to evaluate different control strategies in a vehicle, with physical dynamics and components with nonlinear behaviour, limitations and delays. The size was chosen to be 1/6 scale and effort has been spent on finding suitable components such as off the shelf exchangeable parts.

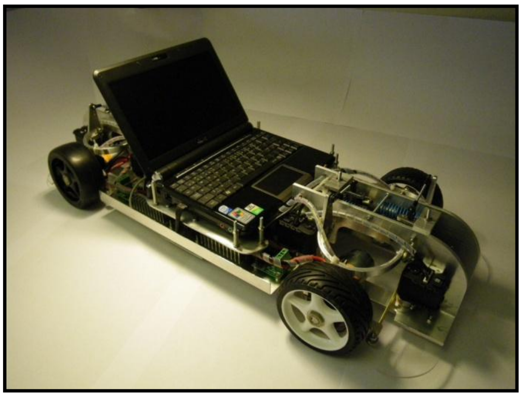

Figure 3.1. The prototype vehicle “Hjulia” with autonomous corner module functionality.

Example of other down-scaled vehicles is the Scale Model Car (SMC) [18] used for hybrid drive line control and education. One advantage of Hjulia is that it is intended to be driven on a non moving surface, unlike most other scale vehicle solutions [19-20], where the vehicles are driven on a moving track or roller which has its own dynamic behaviour, especially influencing the longitudinal dynamics.

Hjulia has no mechanical links between the wheels and has the ability to control each of the wheels individually. It is inspired to as closely as possible enable the functionality of the ACM concept [10-12]. Each wheel is controllable in 4 DOF; wheel rotation, steering angles, camber angles and vertical wheel force/position are made controllable, see Figure 3.2. Weight and dimensions of Hjulia is presented in Table 3.1.

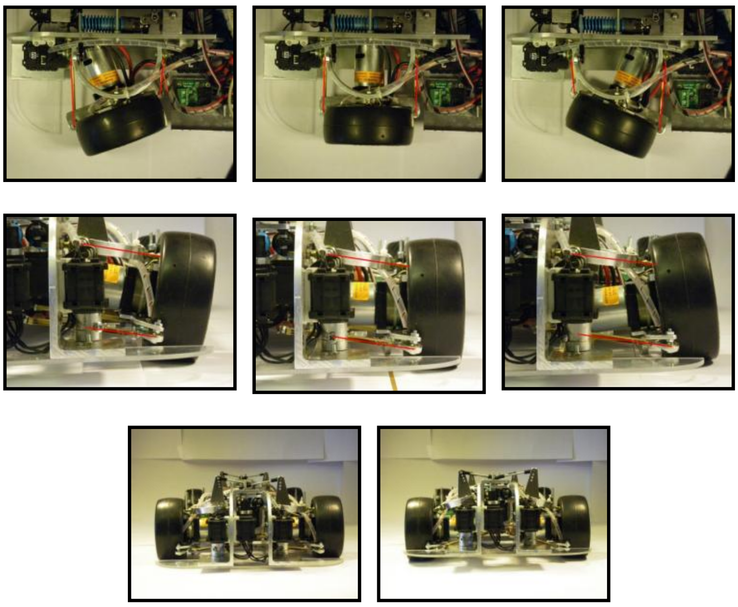

Figure 3.2. Steering, camber and vertical wheel adjustment.

Table 3.1. Weight and dimensions of Hjulia.

Mass	~12 kg
Yaw Inertia	0.7 kgm^2
Wheel base	0.45 m
Width	0.25 m
Height	0.14 m
Wheel size	Ø 0.1 m

At each wheel corner of Hjulia there are three actuators attached that together with the wheel motor will control a total of 4 DOF of each wheel. The actuators (Robotis AX-12 [21]) are controlled via a serial TTL-bus. The wheel motors are brushed DC .05 size motors with planetary gearboxes. The speed controllers consist of two dual motor drivers with regenerative braking ability (Dimension Engineering Sabertooth 2x25 [22]).

The wheels on Hjulia are the same size and have the same hub-to-rim attachment as on radio controlled 1:8 off road racing buggies, with high availability of "off the shelf" wheels and tyres. The actual size of the wheels however scales better to 1:6 rather than 1:8 if the wheel-size to vehicle-size ratio is considered. The tyre used in these studies is a foam tyre with isotropic and smooth characteristics. For more information about the scaled vehicle see **Paper A**.

3.1 Measurement equipment

In order to be able to measure tyre characteristics and to calibrate the wheel speed controllers a roller rig was built, see Figure 3.3. It is designed as a very simple rig fixing one axle of the vehicle to the rig. Under the other axle there is a roller with high inertia. This inertia is coupled to the vehicle as the tyres of the active axle are rolling on the surface of it. The inertia of the roller corresponds to an imaginary vehicle weight of 6 kg.

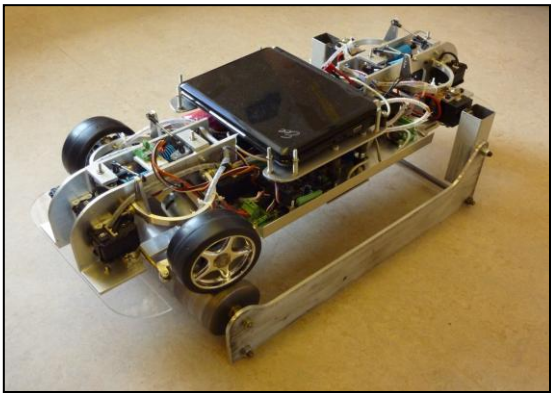

Figure 3.3. Roller rig for calibration and testing of wheel controllers.

As mentioned in Chapter 2, scaling of gravity is important to be able to attain a more relevant dynamic behaviour of a scaled vehicle. A solution, proposed in **Paper A**, is to add an additional rig to the vehicle, lifting it close to the centre of gravity, thus reducing the wheel load in order to get more correctly scaled forces. For example the stopping distance as well as elapsed time will be more directly comparable with a full-size vehicle. The dynamics becomes slower and thus the effects of actuator rate limits and loads will be less critical. Therefore a lifting rig to Hjulia was designed and built, see Figure 3.4. The lifting rig is a simple H-frame with caster wheels lifting the vehicle in the centre of gravity. A pulley and pull spring mechanism is used to get a constant lifting force unaffected by the vertical position.

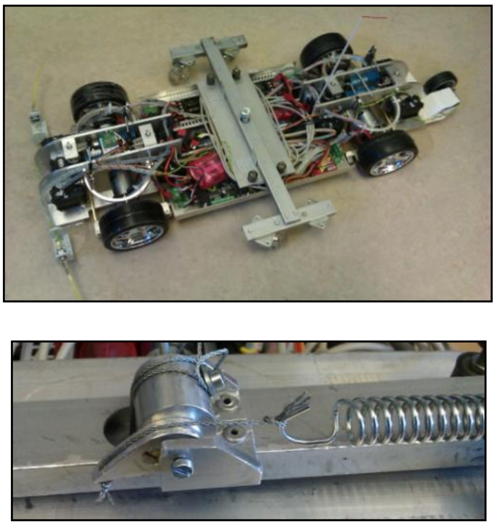

Figure 3.4 Hjulia with lifting rig and the constant force pulley on the lifting rig.

Very critical for all vehicle control systems is the correct estimation of vehicle states. Therefore a large effort within published work in this field is about sensor data processing and estimation of vehicle lateral/longitudinal velocity and yaw rate, as it is required for the vehicle controller to know these states. For example is vehicle speed critical input for an ABS system [23-25], and yaw rate and lateral velocity for chassis controllers [26-27]. In a simulated environment the vehicle states are given, where in a real environment the sensors used for state estimation are sensitive to many kinds of errors.

The vehicle state measurement equipment in Hjulia is built with external measuring wheels, measuring vehicle side slip angles at two points and vehicle speed in one point, see Figure 3.5. The resulting vehicle speed, yaw-rate, position and yaw angle is geometrically calculated using known dimensions and sensor data.

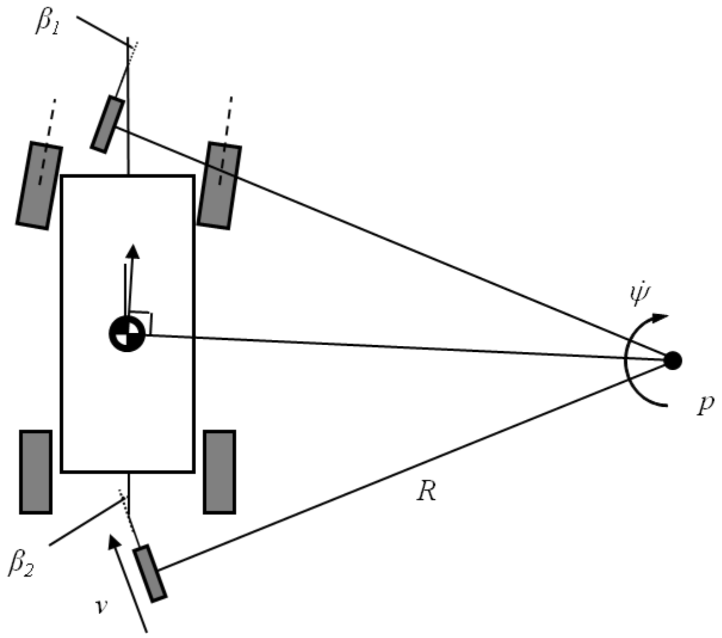

Figure 3.5. Geometric identification of vehicle states from measured trailing wheel angles (β_1 and β_2) and velocity (v), that calculates instantaneous point of motion (p) at the radius (R) from the rear trailing wheel around which the vehicle will rotate around with the yaw rate ($\dot{\psi}$).

3.2 Tyre measurement and modelling

To be able to model the vehicle, the tyres of the prototype vehicle are measured and modelled. Tyre characteristics are nonlinear and are a source of many uncertainties. Therefore it is crucial to know how the tyres behave especially if they are to be compared to full-size tyres. It is also beneficial to know the tyre characteristics for the wheel-slip control.

Longitudinal tyre characteristics are measured using the roller rig. The rig is equipped with a friction brake of belt type where the braking force is adjusted by adding or moving a weight on the bracket, pivoting around point A, see Figure 3.6. The belt brake goes around the roller and a pulley on the bracket. Frictional force generated by the belt is transferred to an analogue dynamometer displaying the actual braking force. Speed of the driven wheel is measured, as is the speed of the roller. The driven wheel is set to a constant speed and the force is measured with the dynamometer. The tyre, which consists of foam rubber glued onto a plastic rim, is measured at different vertical loads and with high and low friction in the tyre/roller contact.

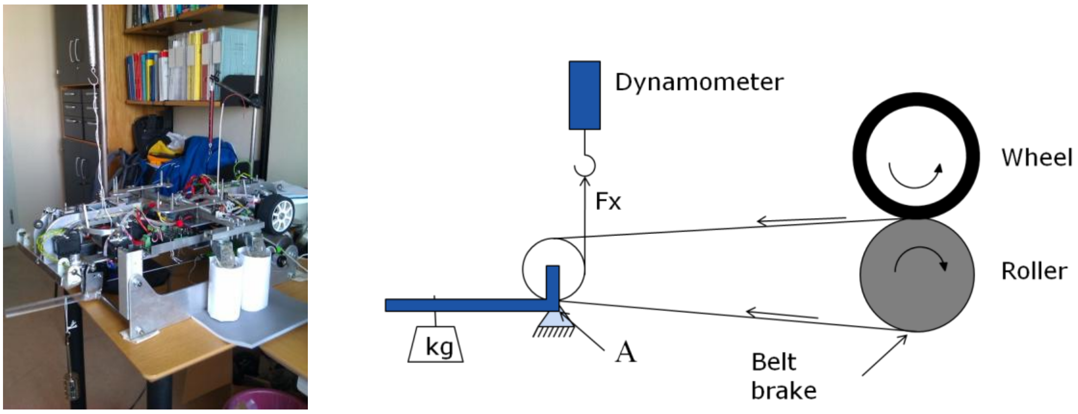

Figure 3.6 Belt brake setup on the roller rig.

Tyre characteristics are modelled using a brush tyre model with constant pressure distribution over the contact patch length. The brush tyre model is a well-known physical model of how a tyre mechanically generates the force as a function of side slip angle and/or longitudinal slip [28].

In the brush model the contact patch length is a critical component in the total tyre stiffness calculation. The contact patch length is depending on the vertical tyre load and on the geometry of the contact patch. When the tyre rolls on a curved surface the tyre contact patch is shorter than on a flat surface. Therefore tyre characteristics measured in the roller rig need to be compensated when running on a flat road. To compensate for the vertical load influence of stiffness, the contact patch length is calculated as a function of vertical load and deformed foam rubber for two different cases; tyre rolling on a roller and tyre rolling on flat ground.

Depending on the geometric relation between tyre diameter and roller diameter the contact area consists of circle segments connecting the contact length to vertical load. The contact area is approximated by a rhombus, where the length corresponds to the contact patch length and the height is given by the wheel and roller geometry. Tyre input data to the modified brush model is given as bristle stiffness, friction coefficient, vertical load and wheel/roller geometry. The bristle stiffness is isotropic in the foam tyre model and thus creates equal vertical and longitudinal stiffness.

To calculate the contact patch length at a given vertical load F_z the tyre will deflect as a set of springs where the number of springs in contact increase as the tyre deforms. Tyre vertical deflection is coupled to contact patch length, where the deformed area can be approximated by a triangle for the flat road calculation, see Figure 3.7a, and a rhombus, see Figure 3.7b, for the roller rig case.

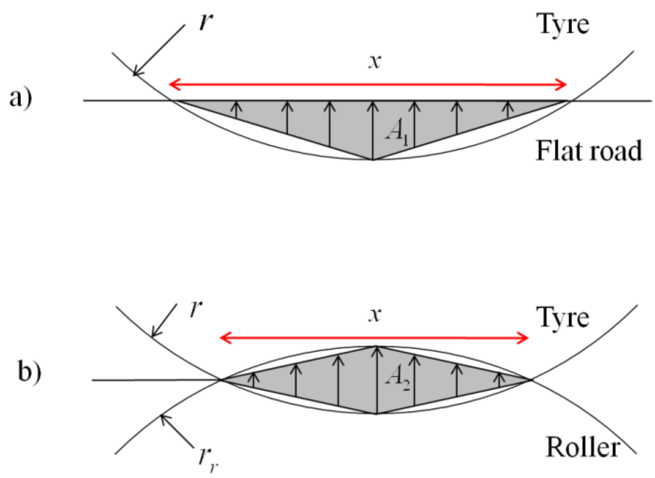

Figure 3.7 Contact patch length and tyre deflection on a) flat road and b) roller rig.

If the tyre bristle stiffness per unit length is cp_z and tyre radius is r the contact patch length can be approximated to be

$$x = \sqrt[3]{\frac{F_z \cdot 16 \cdot r}{cp_z}} \tag{12}$$

for the case of the tyre rolling on flat road. During tyre measurement performed on the roller rig the contact patch length calculation will be approximated to

$$x = \sqrt[3]{\frac{F_z \cdot 16}{cp_z\left(\frac{1}{r}+\frac{1}{r_r}\right)}} \tag{13}$$

where r_r is the roller radius.

Figure 3.8 shows measured results together with the fitted brush tyre model results, modified with the above described load dependency. It can be seen that the tyre model is in good agreement with the measurements.

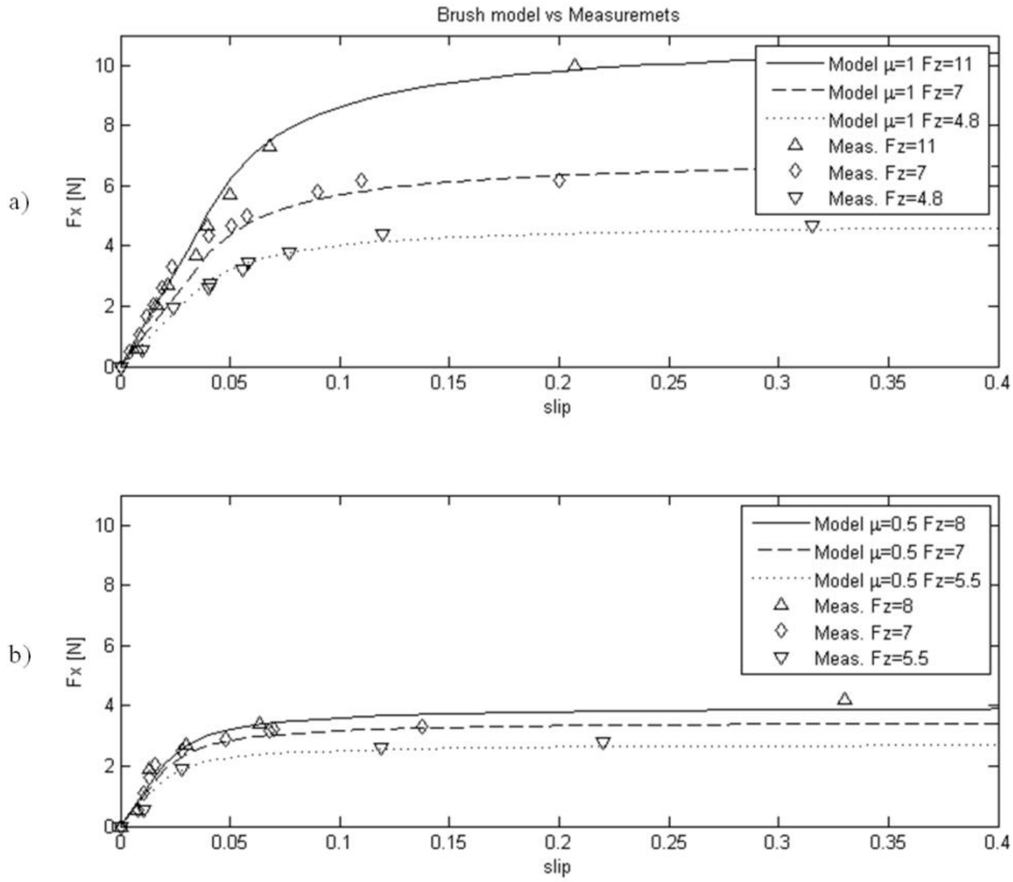

Figure 3.8 Tyre measurement data and brush tyre model characteristics on a roller rig, a) results on high friction surface, b) low friction surface results.

For simulations the contact length calculation in the brush tyre model is changed from rig mode to flat ground mode according to Equations 12 and 13. In Figure 3.9 it is clearly seen that the tyre will behave stiffer on a flat road.

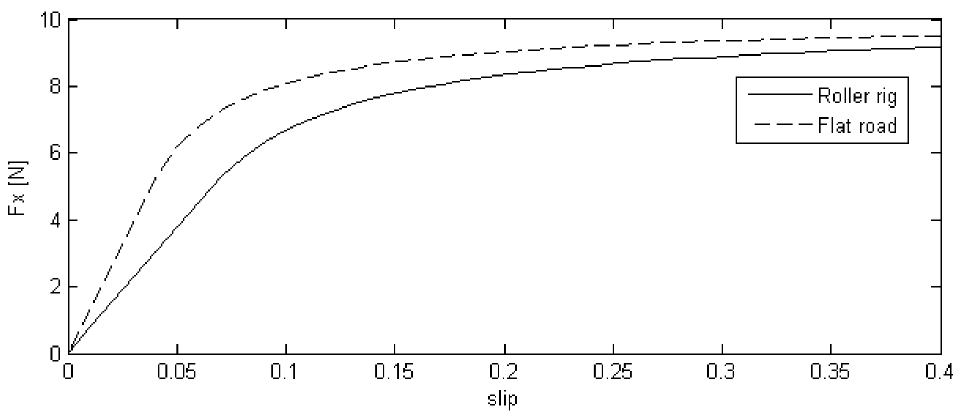

Figure 3.9 Resulting longitudinal tyre characteristics in the roller rig and for flat road contact patch calculation.

The resulting brush tyre model for flat road is used in the simulation model of Hjulia for further analysis and comparison to the down-scaled vehicle tests.

4. Vehicle and force allocation control

To enable force allocation control a controller environment has been implemented in the prototype vehicle. This environment utilises the individual wheels as generic points to apply forces. Driver input signals is given to the onboard computer via a regular radio controller used for radio controlled cars. In the computer, steering and throttle/brake signal is distributed to the steering actuators and wheel motor control signal inputs. For each wheel there is one wheel motor controller, shown in Figure 4.1. Here the requested driving or braking force is sent to the controller. If there is enough friction between tyre and road the wheel motor will generate requested force. If friction is low the so called slip controller is activated limiting the force sent to the motor. Slip control is active during acceleration (traction control) and braking (ABS), working to limit the longitudinal slip of the wheel within a pre set limit. Necessary sensors for this is wheel speed ω_{wheel}, motor current I and battery voltage U. If slip control is active the force is also sent back to the chassis controller. The control output is the duty cycle (1-100%) giving the requested voltage as a percentage of the battery voltage.

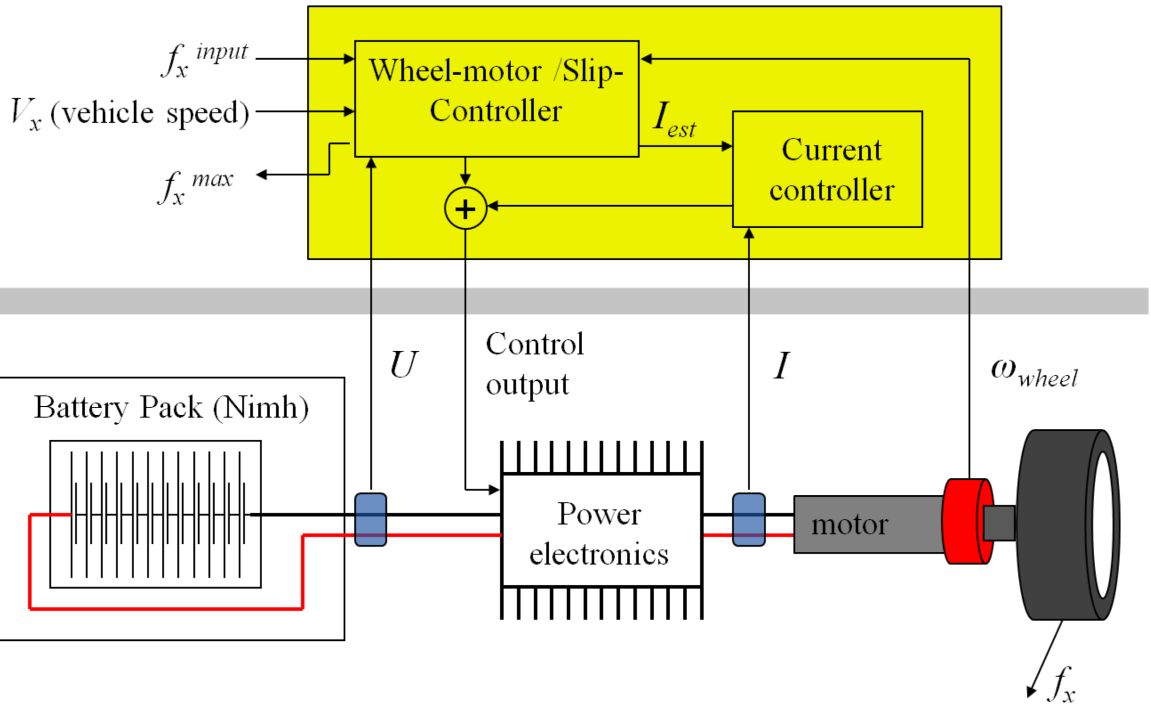

Figure 4.1. Schematic view of the wheel motor drive and control system.

Figure 4.2 show the four individual wheel motor controllers included in the vehicle control system. In this case the yellow box contains the force allocation algorithm.

In the simplest case the longitudinal force signal f_x is fed directly through and divided equally to all four wheels.

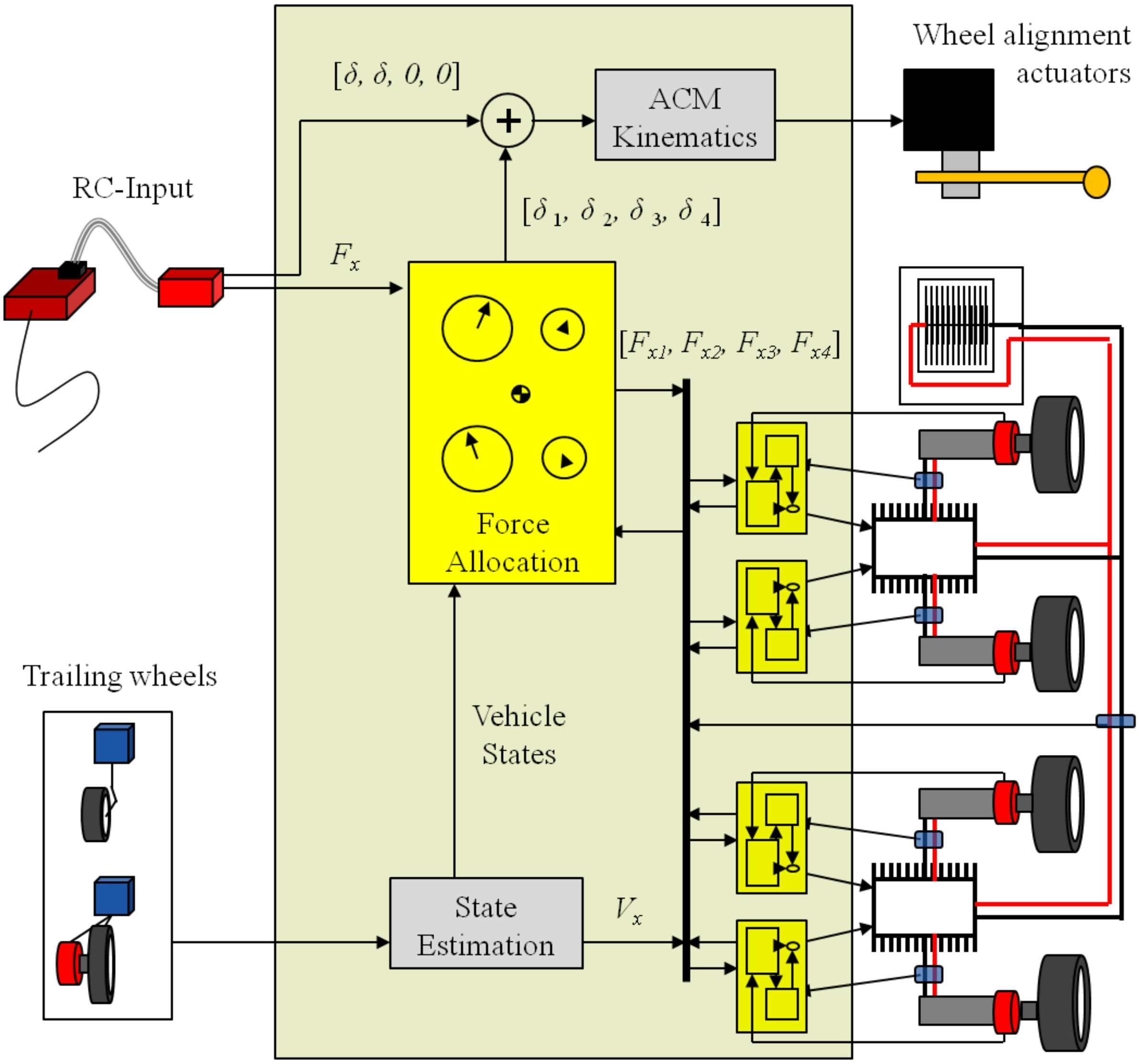

Figure 4.2 Schematic view of the vehicle controller for the down-scaled vehicle.

4.1 The force allocation algorithm

The cost effective force allocation algorithm implemented in Hjulia relies upon simplified assumptions of constraints at each wheel that results in a fast and direct algorithm with few sensors. The input of global forces (F_x, F_y) and global yaw torque (M_z) is distributed onto the four corners of the vehicle. Three different solutions from one global input force each is calculated and added together. The problem is easy to solve if the constraints in attainable wheel forces is not considered. The force allocation method applied here is inspired upon the principle of force allocation presented by [29-32], but is extended with the ability to deal with basic constraints. The constraints will, in this case, be given by the maximum brake force levels from the wheel slip controller. They are recalculated into four normalized values representing the different amount of distributed force attainable at each wheel. Visualized in Figure 4.3, the size of the circles corresponds to these values.

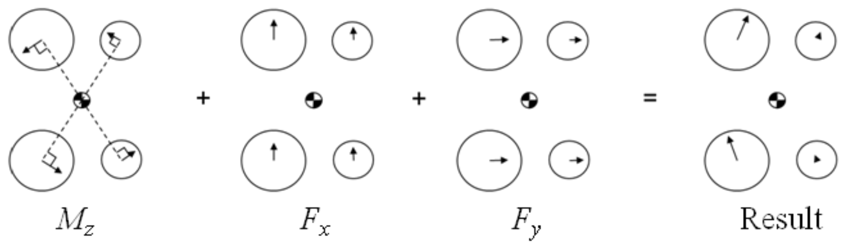

Figure 4.3. An illustration of the applied force allocation algorithm.

The algorithm takes the yaw torque input and distributes it on the four corners so that each force vector is orthogonal to the lever arm from the centre of gravity to the corner and the magnitude is determined by the normalized normal force distribution. It then continues to add the longitudinal and lateral inputs in the same way as for the yaw torque. The error in global force is fed back and the algorithm will loop until the resulting global output corresponds to the input. For more details about this algorithm see **Paper B**.

The corner forces given by this force allocation approach is then recalculated into the wheel coordinate system as longitudinal wheel force and steering angle via an inverse tyre model based on linear tyre stiffness.

For the case of straight line μ-split braking, commonly used for testing stability of controllers [33], the yaw torque input is zero. Split-μ braking occurs when the tyre/road friction is different on each side of the car, for example when driving over a patch of water or ice. The differences in longitudinal forces will result in a yaw torque that the force allocation algorithm will compensate for by individual steering. The conceptual wheel force distribution during μ-split braking is shown in Figure 4.4.

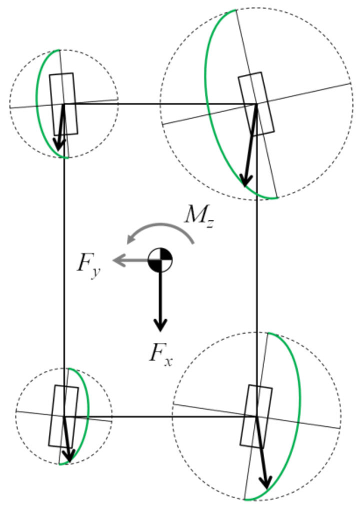

Figure 4.4 Illustration of wheel force distribution during μ-split braking. The yaw torque, given from the differentiated brake forces, is compensated by individual steering, giving no lateral force (F_y) or yaw torque (M_z). The green half circles corresponds to the possible force attainable at a given slip angle.

4.2 Experiment and simulation results

To evaluate the force allocation control approach in Hjulia, experiments are performed with the vehicle. The chosen manoeuvre is straight line braking on μ-split with the left hand side wheels running on lower friction. To acquire lower friction coefficient the left hand side wheels are covered with tape. Three different settings are tested. Setting A is equipped with only individual wheel slip controllers (ABS). Setting B is extended to equalise the brake force on each axle, by choosing the lowest acquired braking force to both wheels. Setting C is equipped with the force allocation algorithm presented earlier that at any given situation redistribute wheel forces so that the global force acting on the vehicle chassis is as the requested input. In this case the induced yaw torque, due to differentiated brake force distribution, is compensated for by steering the wheels individually so that the total yaw torque on the vehicle remains zero. Figure 4.5 show the schematic view of the three settings and how tyre forces contribute to global forces.

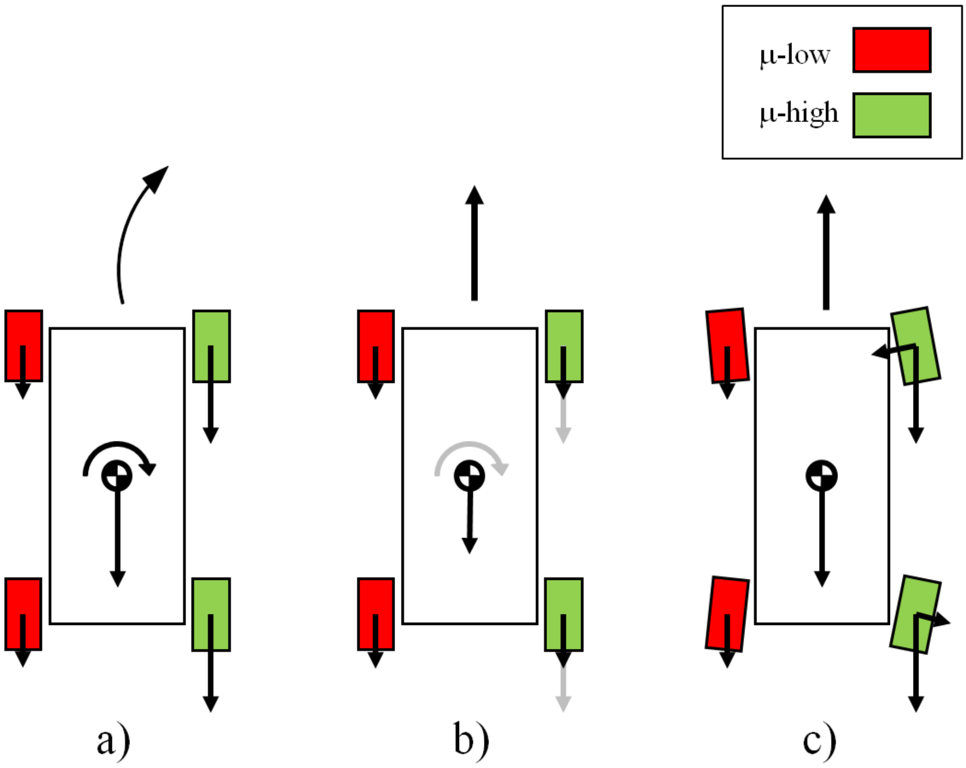

Figure 4.5 Vehicle under braking on μ-split. a) maximised braking on all wheels, b) axle-wise equal braking force and c) yaw torque compensated braking using the force allocation algorithm and individual four wheel steering.

The measurements shown in Figure 4.6 are illustrating the stopping distance from the three settings. To evaluate the experimental results a 10 DOF simulation model using the tyre model in Section 3.2 is implemented with the same control algorithm as described above. Figure 4.7 shows simulation result of the same manoeuvre. Results show that Setting C, implemented with force allocation control has the shortest stopping distance in both simulations and experiments. More information on results, description of the simulation model and the vehicle controller can be found in **Paper B**.

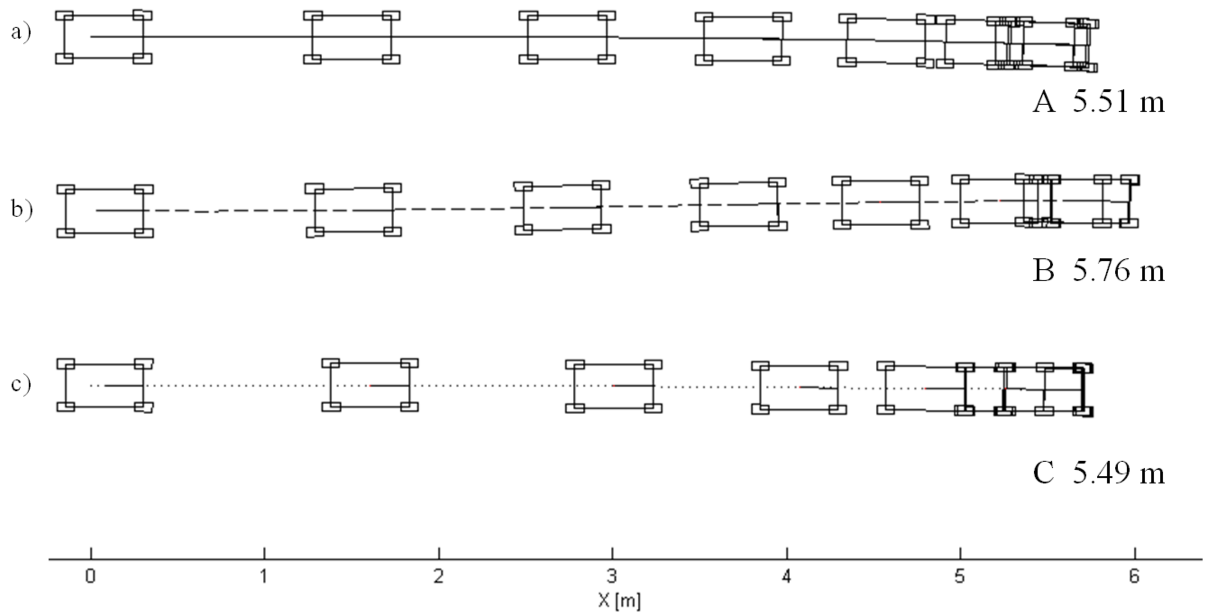

Figure 4.6 Resulting path from the experiment for the three vehicle configurations. a) Path from Setting A. b) Path from Setting B. c) Path from Setting C.

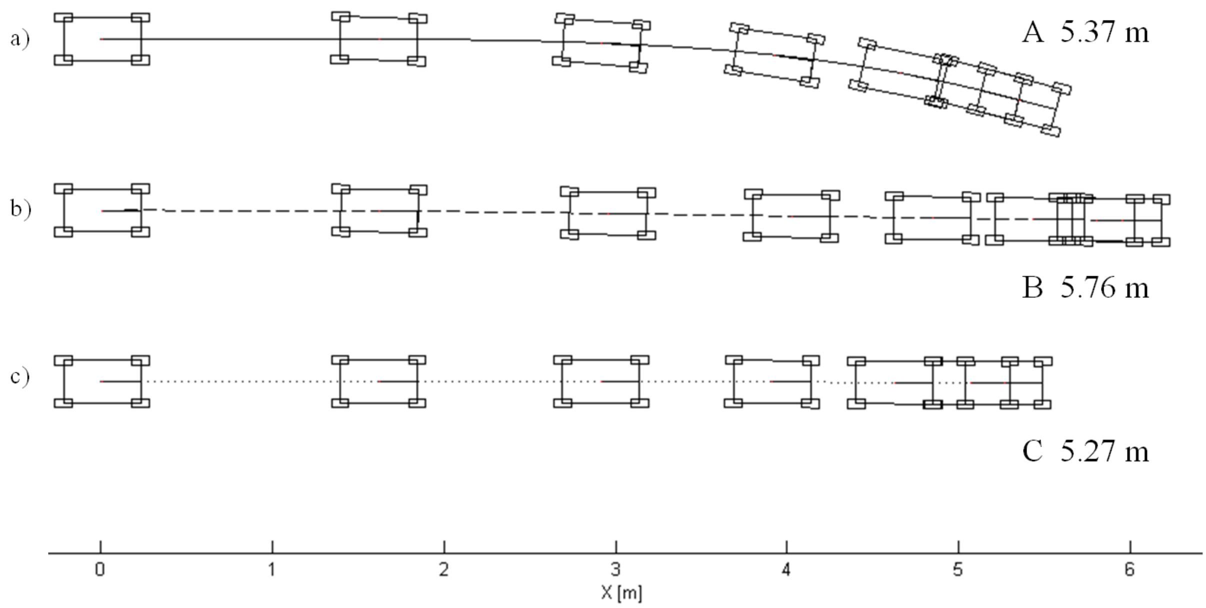

Figure 4.7 Resulting vehicle path from simulated split-μ braking. a) Path from Setting A. b) Path from Setting B. c) Path from Setting C.

5. Optimal vehicle control analysis

5.1 Background

In the process of control systems design it is very useful to also be able to analyze driver and vehicle behaviour. A high skilled driver is very good at using the vehicle dynamics knowledge to maximize the friction utilisation and also to find an optimal path to follow. Often is the control strategy in vehicle stability systems different in how they maintain vehicle stability, compared to how a high skilled driver would have handled the same situation. Using optimisation is one identified approach that gives interesting insight in the problem. A solution of a vehicle controlled by an optimisation algorithm is one way to obtain results that is not inhibited by any predefined controller. Available in the JModelica.org platform [34] there are tools to set up a problem of optimal vehicle control to negotiate path tracking or obstacle avoidance. Other studies involving optimisation of vehicle control can be seen in [35-38].

This chapter will discuss the possibilities of studying vehicle control optimisation. In **Paper C,** this approach is chosen to analyse different manoeuvring strategies at low friction surfaces, as friction is one of the biggest uncertainties, to study if there is any difference in how a vehicle should optimally be controlled regarding friction level. The optimisation algorithm can be given the ability to calculate any number of actuator control signal outputs, which makes this solver a powerful tool to study over actuated systems.

5.2 Vehicle model for the optimisation study

The vehicle model used by the optimisation solver is described with 6 DOF to represent the motion of the vehicle body, see Figure 2.1. The tyres are modeled with basic magic formula description for pure slip conditions [17], without taking wheel spin into account. Longitudinal forces are used directly as input to the tyre model, with limitations in vertical wheel load and friction.

Parameters for the vehicle model are the same as for the full-size vehicle in Table 2.1. In Table 5.1 the actuator constraints are defined.

Table 5.1: Conceptual constraints

Actuator system	Constraints
Friction Brakes	$T_i > -\infty$ Nm, -25 kNm/s < dTi/dt < 7.5 kNm/s, i = 1, 2, 3, 4
Front Axle Steer	$-45° < \delta_{\text{front}} < 45°$, $-75°/s < \delta_{\text{front}}$ /dt < 75°/s

5.3 Optimisation method

The optimisation problem is formulated to maximise entry speed when entering a safety-critical manoeuvre without departure off the road or collide with obstacles. With an increased manageable entry speed, vehicles in real-life traffic would be able to manage critical situations better if one is assuming a certain frequency distribution of speed.

To facilitate the convergence of the optimisation process, the friction usage η for each wheel i is added to the optimisation problem. The optimisation formulation includes actuator constraints and also friction constraints on longitudinal tyre force inputs. The problem formulation also includes constraints on vehicle position expressed in the inertial system. This is used to secure that the vehicle will not leave its lane. Permitted regions in global positions are designed by defining forbidden regions using polynomials. A test manoeuvre with cones to mark permitted regions has been used. Each cone n capture a forbidden region expressed as

$$Y \geq Y_{cone,n} + \left(k\left(X - X_{cone,n}\right)\right)^2 \tag{18}$$

where X, Y are inertial coordinates for the forbidden region associated with the n^{th} cone positioned at cone coordinates ($X_{cone,n}$, $Y_{cone,n}$). k ($k=0.3$) is the shape factor of the polynomial. Only vehicle centre of gravity (CoG) coordinates are considered when formulating path constraints. Therefore locations of cones and curve edges are adjusted with the width of the vehicle to keep the manoeuvre definitions as true to reality as possible. This is all described separately from the model using an extension of the Modelica language within the JModelica.org platform called Optimica [34, 39], that allow for the problem to be described in a convenient and intuitive way.

5.4 Test setup

The goal of the optimisation is to maximise the initial velocity, giving a solution that can be considered to solve a safety critical task. Therefore the solution of actuator control signals tends to often saturate the constraints of the actuators.

The Consumer union double lane change manoeuvre [40] is selected as an inspiration of the definition of the test manoeuvre to evoking over steering. The test is performed by driving the vehicle through a vehicle lane marked by a number of cones, positioned in global coordinates as illustrated in Figure 5.1. This manoeuvre evaluates the vehicle's ability to carry out avoidance manoeuvres, typically appearing where an obstacle suddenly appears in front of the vehicle. The vehicle dynamics problem which sets the limit is generally over steering, i.e. that the vehicle loses side grip on the rear axle and becomes unstable. The constraints of vehicle position throughout the manoeuvre described by Equation 18, is shown around two of the critical cones for this manoeuvre.

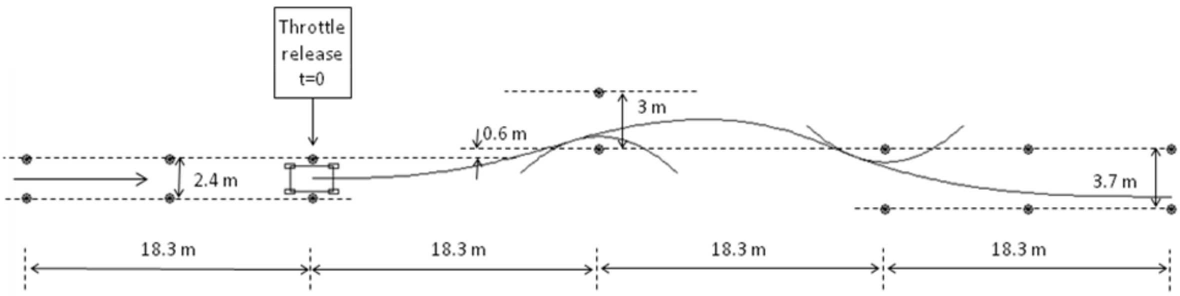

Figure 5.1 Definition of the evasive manoeuvre.

The optimisation starts when CoG of the vehicle is in the position marked 'throttle release' in Figure 5.1. At this position the vehicle is centred between the cone pairs and is directed with zero yaw angle, zero yaw rate and zero lateral velocity. This initial condition has been selected since it is most likely that a driver in a real life situation is not well prepared that an evasive manoeuvre is to occur. For more details, see **Paper C**.

5.5 Results

In Figure 5.2 the resulting optimal global path can be studied for high friction contact situation.

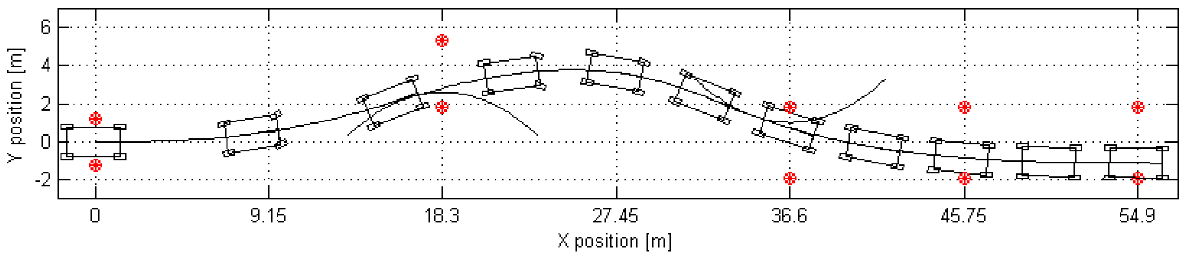

Figure 5.2 Resulting optimal path of vehicle position for high friction situation.

Figure 5.3 show the global acceleration levels and yaw torque of the vehicle. Here it can be seen that the solution start with hard braking maximizing friction utilization until the lateral acceleration builds up. At around 30 m the car is no longer required to drive at the limit.

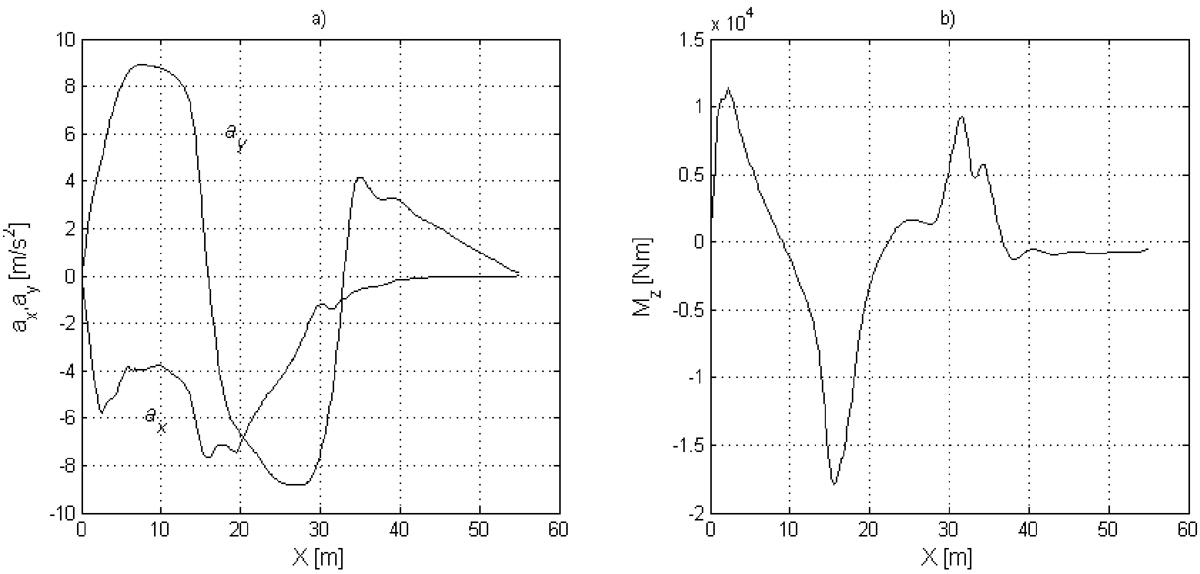

Figure 5.3 Optimisation results of evasive manoeuvre on high friction situation. Plots on vehicle global force level showing a) vehicle longitudinal acceleration (a_x), lateral acceleration (a_y), and b) vehicle yaw torque (M_z).

Figure 5.4 show the longitudinal tyre forces and steering angles. The build up of brake forces is from the beginning restricted by brake actuator limits. Note that relatively large braking forces occur at the rear axle, leaving the front wheels to be able to steer and build up lateral forces. The difference between the left and right rear braking force can be explained by the load transfer onto wheel 4 in the beginning of the manoeuvre. Steering actuation is more or less saturated at all times. First at steering rate limit until max steering angle is reached, then at opposite steering rate limit until max opposite steering angle is reached. At around 30 m the car is no longer required to drive at the limit and the actuator signals are more relaxed.

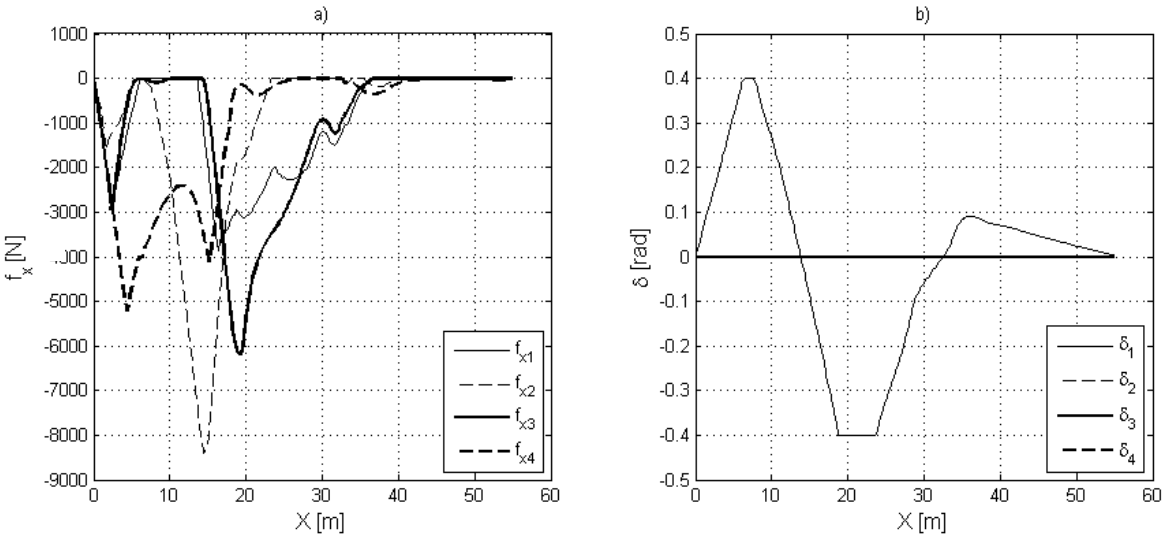

Figure 5.4 Optimisation results of evasive manoeuvre on high friction situation. Plots on actuator entity level showing a) longitudinal tyre forces (f_{xi}) and b) steering angles (δ_i) at each wheel, respectively.

Figure 5.5 show a visualisation of the vehicle at different points in the manoeuvre. Note that the thicker lines visualises the vertical load on each wheel. Brake actuation on the rear is initially fairly large and basically saturates the rear tyres since force potential of the rear wheels is low due to the forward load distribution under braking.

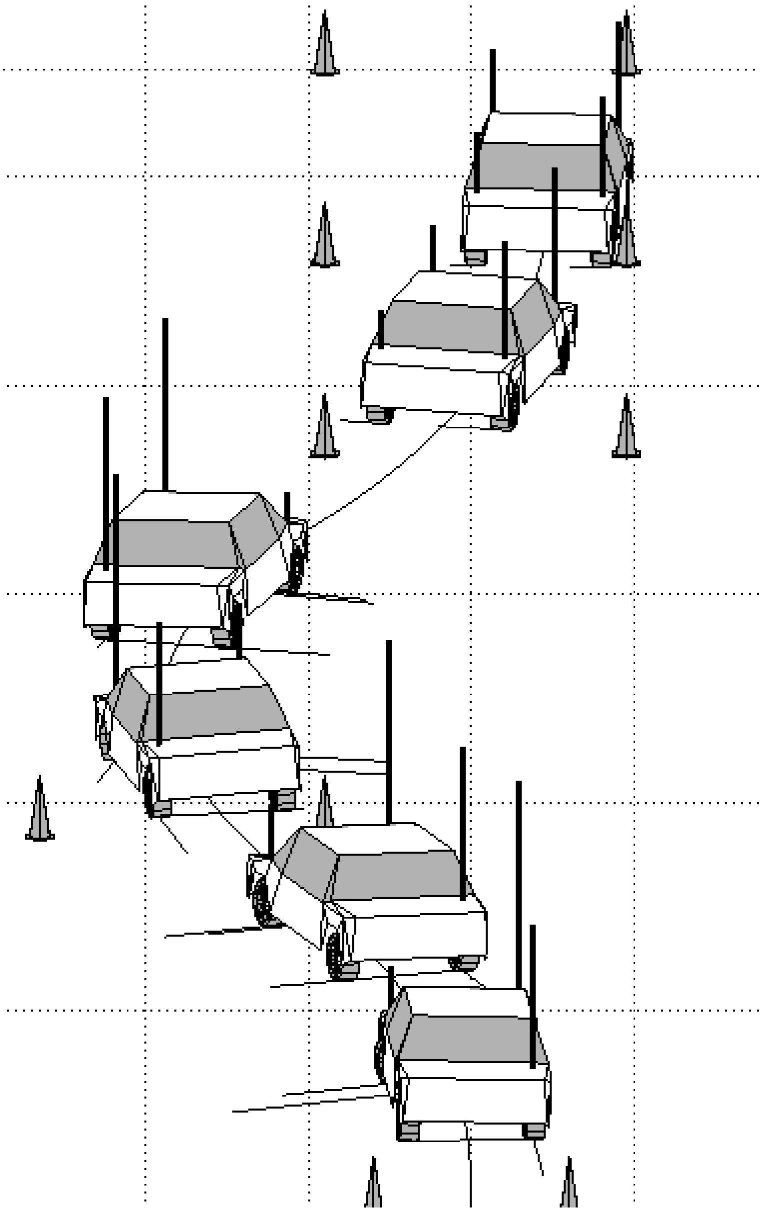

Figure 5.5. Visualisation of the optimized vehicle solution on high friction situation.

It can clearly be seen that actuator limits play a major role in the resulting solution, especially at high friction situation where vehicle speed and acceleration will be high. In **Paper C** which includes results also at lower tyre/road friction, shows that the results are less limited by actuator limits. **Paper C** also contains results with a vehicle with additional rear axle steering, showing improved performance in how fast the vehicle can respond.

6. Summary of appended papers

Paper A: "The development of a down-scaled over-actuated vehicle equipped with autonomous corner module functionality"

In this paper, the development of an over-actuated down-scaled vehicle (Hjulia) is presented. It is designed to study drive by wire systems where many different aspects are to be considered, such as actuator limitations, signal processing and advanced control algorithms. The use of a scale prototype vehicle represents a compromise between cost efficiency and accuracy, as it allows realistic experiments without the cost and complexity of full vehicle test. Other benefits is that when studying vehicle behaviour at-the-limit, a down-scaled vehicle presents much smaller risks of mechanical damage and human injury, and needs far less costly infrastructure to be able to run tests. The mechanical design to enable an over-actuated vehicle platform together with the hardware layout of the control system is described. It is equipped with *autonomous corner module* functionality that enables full individual control of all wheels, regarding steering, camber, propulsion/braking and vertical loads. This results in a down-scaled prototype vehicle to be used for future vehicle dynamic research for evaluating different control approaches, including the sensitivity to actuator limitations and response times.

Paper B: "Force allocation control of a down-scaled prototype vehicle"

This paper describes control implementation and experiments using the down-scaled prototype introduced in **Paper A**, in order to evaluate force allocation control in an at-the-limit situation. For this, controller system design, vehicle state estimation with trailing wheels and a lifting rig to emulate a lower gravitational pull for more full-size comparable results, is described. A fast, cost effective force allocation algorithm is proposed and implemented. This force allocation algorithm utilises simplified constraints in order to compensate for the different amount of attainable force at each wheel, that is the result of different friction level and wheel load distribution. The algorithm is running "on-line" meaning that it is fast enough to calculate the appropriate force distribution in real time without excessive computational power. The controller is evaluated in a split-μ scenario, where the performance of the force control allocation algorithm is studied, during hard braking. This is done both in the real experiments and in a simulated environment with a simplified vehicle model. The result shows that there is high potential in using force allocation to improve vehicle performance.

Paper C: "Road friction effect on the optimal vehicle control strategy in two critical manoeuvres"

To be able to find new control methods to utilise the increase of actuators in vehicles, this paper describes a methodology used for solving actuator control signals for vehicles in two different critical driving scenarios (Double lane change and J-turn), using optimisation to maximise the input velocity of the vehicle. Actuator configurations studied are enhanced front axle steering and individual brake actuation, as well as a vehicle with additional rear axle steering. Special focus is on how control output behaviour is depending on wheel to road friction level. Results show that the amount of load transfer is strongly depending on acceleration levels, and thus friction levels. Actuator constraints will be less critical on low friction surfaces due to lower force levels and a lower speed. Force distribution on wheel level show different behaviour between the low and high friction situation, while global forces scale to the friction coefficient and show a similar behaviour on both high and low friction. It is shown that actuator constraints is influencing the results substantially when high speed and high force levels occurs.

7. Scientific contribution

The main scientific contributions in this thesis can be summarised as follows

1. A decomposition of the complex design of an ACM vehicle was developed to obtain full ACM functionality, **Paper A**. To reduce testing complexity and product cost, the decomposition process resulted in a novel prototype of a down-scaled over actuated vehicle. The prototype has been designed with a control architecture that enables force allocation, **Paper B**.

2. A cost effective force allocation control approach has been implemented and evaluated on the prototype vehicle, as well as in vehicle simulation. Results show improvement of stopping distance and vehicle stability of a vehicle during split-μ braking. In **Paper B** the low cost approach of force allocation is described.

3. Analysis of optimal vehicle behaviour on different friction levels using optimal controller, show that the solutions strongly depend on friction level. Actuator limitations are critical, especially for evasive manoeuvres such as double lane change, **Paper C**.

8. Recommendations for future work

The down-scaled vehicle has shown a potential to evaluate advanced vehicle controllers in different driving conditions and manoeuvres. The functionality of the vehicle can be utilised further since the controller described in this thesis only have implemented control of steering angles and traction/braking of the wheels. One area to improve further is wheel slip control that utilises the new actuator technologies better. The vertical wheel load and camber control are domains of control that are left to explore.

Tyre measurement and modelling is also an area of interest. For example to equip the chassis with further sensors to be able to fully measure the individual tyre force levels will make this vehicle to a powerful platform for tyre testing and thus also improve the vehicle behaviour in how to utilise the tyres. Actuator limitations has been shown to be of great importance, and further studies focusing on at-the-limit control, and how real actuator limits effect vehicle performance, are recommended.

Using optimisation is a very useful approach, but it however relies on simulation models, so an investigation of different models is recommended. The case of controlling the vertical wheel forces is an area of great interest, as the implementation of active or semi-active suspension is already implemented to a high degree in many vehicles. Different actuator configurations are easy to study, to evaluate if there is any major gain in implementing full over actuation. A normal, only brake actuated vehicle can be compared with a full over actuated vehicle and all the different states of actuation in between, for example a common electric hybrid vehicle (HEV) with electric driven rear axle. The cost function will strongly influence what kind of solution the solver will calculate. With this tool there is no limit to the amount of different actuator configurations that can be studied.

9. Concluding remarks

The work presented in this thesis is aimed to make further steps in the progress of over actuated electric vehicles. Especially in the way these new chassis configurations can be controlled with individualised control of each wheel.

This work has been approaching force allocation methodology from both simulation studies using optimisation and real vehicle control implementation. Tools used are a purposely developed scaled prototype vehicle and vehicle simulation optimisation. The scale vehicle is built as a test bench and includes most of the areas that needs to be considered when implementing real vehicle control, such as actuator limits, non ideal sensors and vehicle state estimation.

It is shown that optimisation is a powerful tool when studying over actuated systems. It gives insight in how different actuator configurations perform in different situations. It will also give knowledge to how to design controllers that is able to control vehicles better in both at-the-limit situations and normal non-critical driving.

With a cost effective force allocation approach, both experimental and simulation results show improved performance for the scale vehicle developed in this work (**Papers A** and **B**). This vehicle is built as a research platform and can accommodate control of even further actuator configurations such as camber control and wheel load control, without neglecting sensor uncertainties, tyre characteristics and friction. In **Paper C** it was concluded that actuator performance have a large influence of vehicle performance, especially at high tyre/road friction and high speed situations. The performance is strongly affected by tyre/road friction, vehicle speed and acceleration, since this leads to different load distribution which relate directly to potential tyre forces. Tyre characteristics are always critical for vehicle dynamic studies due to the fact that tyres are non-linear, especially at the limit. The built prototype vehicle with implemented force allocation control will be used for future research in exploring the benefits of force allocation control.

References

[1] http://www.autosavant.com/2008/10/02/hybrid-history-part-one-the-very-early-years/ accessed in October 2011.

[2] J. Andreasson, C. Knobel and T. Bünte, "On road vehicle motion control-striving towards synergy", In Proceedings of 8th International Symposium on Advanced Vehicle Control, AVEC'06, Taipei, Taiwan, 2006.

[3] D. A. Crolla and D. Cao, "The impact of hybrid and electric powertrains on vehicles dynamics and control systems", IAVSD 2011, 22nd international Symposium on Dynamics of Vehicles on Roads and Tracks, 14-19 August, Manchester, UK, 2011.

[4] T. Weiskircher, J.E. Diang and S. Müller, "Control performance and energy consumption of an electric vehicle with single-wheel drives and steer-by-wire", IAVSD 2011, 22nd international Symposium on Dynamics of Vehicles on Roads and Tracks, 14-19 August, Manchester, UK, 2011.

[5] H. Niederkofler, A. E. R. Rojas and J. Dürnberger, "Development of a single wheel steer-by-wire system: Implementation aspects and failure handling", IAVSD 2011, 22nd international Symposium on Dynamics of Vehicles on Roads and Tracks, 14-19 August, Manchester, UK, 2011.

[6] M. Burckhardt, "Erfahrungen bei der konzeption und entwicklung des merschedes-Benz/Bosch ABS", ATZ *Automobiltechnische Zeitschrift*, 1979.

[7] A. Müller, W. Achenbach, E. Schindler, T.Wohland, and F.-W. Mohn, "Das neue fahrsicherheitssystem electronic stability program von Mercedes_Benz", ATZ *Automobiltechnische Zeitschritf*, Vol. 11, No. 11, pp. 656-670, 1994.

[8] M. Jonasson and O. Wallmark, "Stability of an electric vehicle with permanent-magnet in-wheel motors during electrical faults", The World Electric Association Journal, Vol. 1, pp. 100-107, 2007.

[9] M. Jonasson and O. Wallmark, "Control of electric vehicles with autonomous corner modules: implementation aspects and fault handling", International Journal of Vehicle Systems Modelling and Testing, Vol. 3, No. 3, pp. 213-230, 2008.

[10] S. Zetterström, "Vehicle wheel suspension arrangement", Patent No EP1144212, 1998.

[11] S. Zetterström, "Electromechanical steering, suspension, drive and brake modules", Proceedings of IEEE 56th Vehicular Technology Conference, vol. 56, no. 3, pp. 1856-1863, September 24-28, 2002.

[12] M. Jonasson, S. Zetterström and A. Stensson. Trigell, "Autonomous corner modules as an enabler for new vehicle chassis solutions", FISITA Transactions 2006, paper F2006V054T, 2006.

[13] J. Andreasson, "On generic road vehicle motion modelling and control", PhD thesis in Vehicle Engineering, KTH Royal Institute of Technology, TRITA-AVE 2006:85, January, 2007.

[14] M. Jonasson, " Exploiting individual wheel actuators to enhance vehicle dynamics and safety in electric vehicles ", PhD thesis in Vehicle Engineering, KTH Royal Institute of Technology, TRITA-AVE 2009:33, September, 2009.

[15] A. Jaschinski, H. Chollet, S.D. Iwnicki, A.H. Wickens and J. Von Würzen, "The application of the roller rigs to railway vehicle dynamics", International Journal of Vehicle System Dynamics, Vol. 31, pp. 371-373, 1999.

[16] MATLAB and Simulink, registered trademarks of The Mathworks, Inc., Natick, Massachusetts, USA. 2011.

[17] H.B.Pacejka "Tyre and vehicle dynamics", Buttherworth-Heinemann, 2005.

[18] L. Laine, J. Hellgren, H. Kinnunen and M. Rönnerg, "Reusable control architecture implemented in a scale model of a hybrid electric vehicle", Proceedings of Electric Vehicle Symposium (EVS) 21, Monaco, 2005.

[19] S. Brennan, M. DePoorter, and A. Alleyne, "The Illinois roadway simulator—A hardware-in-the-loop testbed for vehicle dynamics and control", in Proc. 1998 American Control Conf., Philadelphia, PA, June, pp. 493–497, 1998.

[20] S. N. Brennan. "Modeling and control issues associated with scaled vehicles", Master's thesis, University of Illinois at Urbana Champaign, USA, 1999.

[21] Steering actuator: Robotis Dynamixel AX12. *http://www.robotis.com/zbxe/dynamixel_en*, accessed in May 2011.

[22] Motor controller: Dimension Engineering sabertooth 2x25. *http://www.dimensionengineering.com/Sabertooth2X25.htm*, accessed in May 2011.

[23] M. Tanelli, S M. Savaresi and C. Cantoni, "Longitudinal vehicle speed estimation for traction and braking control systems", Proceedings of the 2006 IEEE International Conference on Control Applications Munich, Germany, pp. 2790-2795, October 4-6, 2006.

[24] K. Kobayashi, Ka.C. Cheok and K. Watanabe, "Estimation of absolute vehicle speed using fuzzy logic rule-based kalman filter", In Proceedings of the American Control Conference Seattle, Washington, 1995.

[25] A. Daiβ, U. Kiencke, "Estimation of vehicle speed fuzzy -estimation in comparison with kalman-filtering", Control Applications, Proceedings of the 4th IEEE Conference on Control Applications, 28-29, pp. 281-284, 1995.

[26] F. Yoshiki, "Slip-angle estimation for vehicle stability control", International Journal of Vehicle System Dynamics, Vol. 32, No. 4, pp. 375-388, 1999.

[27] A.Y. Ungoren, H. Peng and H.E. Tseng, "A study on lateral speed estimation methods", Int. J. Vehicle Autonomous Systems, Vol. 2, Nos. 1/2, pp. 126-144, 2004.

[28] H.B. Pacejka, “Modelling of the pneumatic tyre and its impact on vehicle dynamic behavior.” Technical Report i72B. TechnischeUniversiteit, Delft, 1988.

[29] J. Andreasson and T. Bünte. "Global chassis control based on inverse vehicle dynamics models". Proceedings of the 19th IAVSD Symposium, Milan, Italy, 2005. Supplement to Vehicle System Dynamics, Vol. 44, 2006.

[30] T. Bünte and J. Andreasson. "Global chassis control based on inverse vehicle dynamics models providing minimized utilisation of the tyre force potential", In Proceedings of Autoreg 2006, VDI Berichte no 1931, 2006.

[31] L. Laine. "Reconfigurable motion control systems for over-actuated road vehicles". PhD Thesis in Applied Mechanics. Chalmers, June 2007.

[32] L. Laine and J. Fredriksson, "Coordination of vehicle motion and energy management control systems for wheel motor driven vehicles", Proceedings of the 2007 IEEE Intelligent Vehicles Symposium Istanbul, Turkey, June 13-15, 2007.

[33] R. G. Hebden, C. Edwards and S. K. Spurgeon , “Automotive steering control in a split-μ manoeuvre using an observer-based sliding mode controller”, International Journal of Vehicle System Dynamics, Vol. 41, No. 3, pp. 181–202, 2004.

[34] JModelica, http://www.jmodelica.org/ accessed in October 2011

[35] A. Nozad, M. Lidberg, T. Gordon and M. Klomp, "Optimal Path Recovery from terminal understeer", IAVSD 2011, 22nd international Symposium on Dynamics of Vehicles on Roads and Tracks, 14-19 August, Manchester, UK, 2011.

[36] J. Kang and K. Yi, " Driving control algorithm of 4wd electric vehicle using an optimal control allocation method", IAVSD 2011, 22nd international Symposium on Dynamics of Vehicles on Roads and Tracks, 14-19 August, Manchester, UK, 2011.

[37] J. Deur, J. Kasać, M. Hancook and P. Barber, "A study of optimization-based assessment of global chassis control actuator configurations", IAVSD 2011, 22nd international Symposium on Dynamics of Vehicles on Roads and Tracks, 14-19 August, Manchester, UK, 2011.

[38] P. Sundström, M. Jonasson, J. Andreasson, A. Stensson Trigell, B. Jacobson. "Path and control optimisation for over-actuated vehicles in two safety-critical maneuvers", AVEC 2010.

[39] Modelica, http://www.modelica.org/ accessed in October 2011

[40] http://www.consumerunion.org/ accessed in October 2011

Nomenclature and glossary

Latin symbols

a_x, a_y, a_z	Longitudinal lateral and vertical acceleration
f_{xi}, f_{yi}, f_{zi}	Longitudinal, lateral and vertical tyre forces
f_{xc}, f_{yc}, f_{zc}	Longitudinal, lateral and vertical corner forces
F_x, F_y, F_x	Longitudinal, lateral and vertical global vehicle forces
M_x, M_y, M_z	Global vehicle roll, pitch, and yaw torques
g	Gravitational constant
h	Height from ground plane to centre of gravity
f, b	Front and rear axle to centre of gravity distance
wb	Track width
J_{xx}, J_{yy}, J_{zz}	Roll, pitch and yaw inertia
m	Vehicle mass
c	Spring stiffness
d	Damping coefficient
s	Longitudinal tyre slip
r, r_r	Wheel radius and roller radius
k	Shape factor of polynomial around cones
$T_{w1}, T_{w2}, T_{w3}, T_{w4}$	Total wheel torque, for each wheel respectively
v_x, v_y, v_z	Vehicle longitudinal lateral and vertical velocities in vehicle coordinate system
X, Y	Vehicle longitudinal and lateral displacement in road coordinate system
p	Point of rotation
R	Radius from centre of gravity to instantaneous point of motion
I	Electric motor current
U	Electric motor voltage
B_1, B_2, B_3, B_4	MF Tyre stiffness, for each wheel respectively
C_1, C_2, C_3, C_4	MF Tyre Shape factor, for each wheel respectively
L_1, L_2, L_3, L_4	Relaxation length, for each wheel respectively
cp_x, cp_y, cp_z	Longitudinal, lateral and vertical tyre bristle stiffness per unit length

Greek symbols

$\alpha_1, \alpha_2, \alpha_3, \alpha_4$	Tyre slip angle, for each wheel respectively
β_1, β_2	Trailing wheel angle for front and rear
$\delta_1, \delta_2, \delta_3, \delta_4$	Wheel steering angle, for each wheel respectively
$\omega_1, \omega_2, \omega_3, \omega_4$	Wheel rotational speed for each wheel, respectively
$\gamma_1, \gamma_2, \gamma_3, \gamma_4$	Wheel camber angle, for each wheel respectively
η	Friction usage
ψ	Vehicle yaw angle in road coordinate system
θ	Vehicle pitch angle in road coordinate system
φ	Vehicle roll angle in road coordinate system
μ	Friction coefficient
φ_l	Length scale factor
φ_t	Time scale factor
φ_ρ	Density scale factor
φ_v	Speed scale factor

φ_a	Acceleration scale factor
φ_m	Mass scale factor
φ_I	Inertia scale factor
φ_F	Force scale factor
φ_T	Torque scale factor
φ_c	Stiffness scale factor
φ_d	Damping scale factor

Subscript and superscript

i	Wheel index
n	Cone index
est	Estimation

Abbreviations

ABS	Anti-lock Brake System
ACM	Autonomous Corner Module
ECU	Electronic Control Unit
ESC	Electric Speed Controller
KTH	Kungliga Tekniska Högskolan
MF	Magic Formula Tyre model
MPC	Model Predictive Control